

Cooperative Optical Wireless Communication: A Perspective of Differential Reliability

Xian Liu

Department of Systems Engineering
University of Arkansas at Little Rock
Little Rock, Arkansas, USA

Changcheng Huang

Department of Systems and Computer Engineering
Carleton University
Ottawa, Canada

Abstract: The performance of *optical wireless communications (OWC)* can be improved by the virtual *line-of-sight (LoS)*. In this study, we consider a paradigm in which the virtual LoS is provided by some *unmanned aerial vehicles (UAVs)*. In the scenario where strong atmospheric turbulence occurs, we derive the formulas of reliability and ergodic capacity. Moreover, we introduce a new protocol to improve the communication reliability. The analysis is conducted in terms of the differential reliability.

Index Terms: Cooperative communication, free space optics, optical wireless communication, relay.

I. INTRODUCTION

The next-generation wireless communication systems will embrace several promising technologies. For example, the *optical wireless communication (OWC)* technology is to play an active role to complement the *radio frequency (RF)* transmissions in several *beyond-the-fifth-generation (B5G)* communication paradigms [1]. Besides the desirable wireless feature, the main advantages of the OWC system are its high channel bandwidth and low device power consumption. Another advantage is the immunization of interference from other devices, due to the very narrower beam of optical signals. However, the signal transmission in OWC is conditioned on the *line-of-sight (LoS)*, i.e. the straight path between the transmitter and the receiver is not obstructed. In practice, the ideal LoS often does not exist. Therefore, some auxiliary means are needed when OWC is to be utilized in the field. One of the promising assistant means is the technology of *unmanned aerial vehicle (UAV)* [2-3]. It is easy to imagine that an appropriately deployed UAV network would provide healthy LoS for participated communication devices. Therefore, it is quite natural to consider a communication paradigm that integrates UAVs into OWC. This paper investigates the benchmark performance of OWC with UAV incorporating some basic *cooperative communication* protocols.

In this hybrid system, we will consider a representative segment (Fig. 1) with a laser device as the source node (S), a UAV as the relay node (R), and an optical receiver as the destination node (D). Accordingly, there are three transmission links: S to R, R to D, and S to D. For convenience, the acronyms *S2R*, *R2D*, and *S2D* are to be used throughout this paper. The cascade S2R and R2D links

are considered as a virtual LoS for the concerned circumstance.

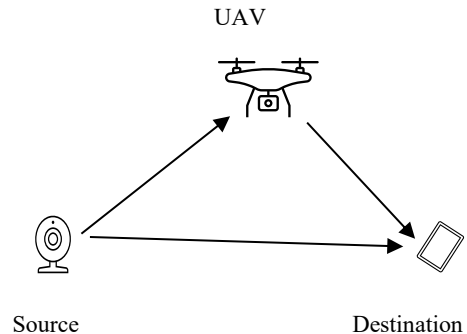


Figure 1. Generic OWC-UAV segment.

The main contributions of the present work come from two aspects. For the concerned system, we derive the formulas of reliability and ergodic capacity. Then, we introduce a new protocol to improve communication reliability. As explored, the analysis involves several advanced special functions. However, most of these functions are supported by popular engineering toolkits such as Matlab.

The rest of this paper is organized as follows. In Section II, the main variables and parameters are listed for convenience. In Section III, the OWC system essentials are described. Then, the basics of atmospheric interference are reviewed in Section IV. A statistical model is introduced in Section V. Next, in Section VI, several relay protocols are reviewed, and a new scheme is introduced. Then, some numerical experiment results are given in Section VII. Finally, Section VIII concludes this paper.

II. NOMENCLATURE

- d_p : link length, e.g., distance between transmitter and receiver, distance between transmitter and relay, or distance between relay and receiver
- C_n^2 : refractive index structure constant
- D_R, D_T : receiver aperture diameter, transmitter aperture diameter
- G_R, G_T : receiver gain, transmitter gain
- h : Plank's constant (6.626069×10^{-34} J · sec.)

- P_R : received optical power without turbulence
- P_T : average transmitted optical power in a symbol period
- q : electron charge (1.602176×10^{-19} coulombs)
- R : detector's responsivity factor (ampere/watt)
- U : instantaneous electrical *signal-to-noise ratio* (SNR)
- U_0 : SNR without turbulence
- η_R, η_T : optics efficiency of the receiver, optics efficiency of the transmitter
- λ : wavelength
- μ : converted electrical current at receiver
- σ_R^2 : Rytov variance
- σ_N^2 : covariance of the *additive white Gaussian noise* (AWGN)

The above list includes main notations only. Other notations are explained where appropriate.

III. SYSTEM DESCRIPTION

In a modern OWC system, each component can have various configurations. Two fundamental modulation methods are on-off keying (OOK), pulse position modulation (PPM). The former is also referred to as *non-return-to-zero* (NRZ) encoding. Each method has some distinct features. A comprehensive review can be found in [4]. In the present work, our analysis is based on a generic system with the following features: (i) on-off keying (OOK) modulation and *intensity modulation* (IM) in transmitter; (ii) *direct detection* (DD) with the *maximum likelihood* (ML) criterion in receiver; (iii) the AWGN noise model described in [4]; (iv) Gaussian beam on the intensity cross section of transmitter; (v) sufficiently wide *field of view* (FOV) in receiver telescope. Other features will be addressed in sequel. In general, we adopt most assumptions and conditions typically recognized in the literature on OWC (e.g., [4], [5]).

According to the Friis transmission equation, the received optical power without turbulence for one particular symbol is:

$$P_R = P_T G_T G_R \left(\frac{\lambda}{4\pi d_p} \right)^2 \eta_T \eta_R. \quad (1)$$

The main parameters in (1) are explained as follows. For the case of Gaussian beam, the transmitter telescope gain is $G_T \approx (2\pi W_0 / \lambda)^2$, where W_0 is the rms width of the Gaussian intensity distribution over the transmitter aperture [6]. The receiver telescope gain can be expressed as [7]: $G_R \approx (\pi D_R / \lambda)^2$. At the detector, P_R is converted to electric current μ . The relation between them can be expressed as $\mu = R P_R$, after removing the background light

[4]. For typical photo-emissive and semiconductor junction detectors, the responsivity is described as $R = R_0 \lambda$, where

$$R_0 = \frac{\eta q}{hc}, \quad (2)$$

c is the speed of light, and η is the detector's *quantum efficiency*, defined as the ratio of the number of emitted electrons to the number of incident photons [8].

IV. MAIN PARAMETERS OF STRONG TURBULENCE

Turbulence is one of the main types of atmospheric interference [9]. Turbulence depends on multiple factors such as altitude, channel length, humidity, and temperature. When turbulence occurs, both amplitude and phase of the received signal randomly fluctuate. So the main impact to OWC is the large deviations of the received signal from its normal strength. Because of its random impacts, in literature turbulence is generally described by stochastic processes. For example, given the distance between the transmitter and the receiver, denoted by d_p , the turbulence can be characterized by the *Rytov variance* [10, p. 323]:

$$\sigma_R^2 = 1.23 \left(\frac{2\pi}{\lambda} \right)^{7/6} d_p^{11/6} C_n^2, \quad (3)$$

where C_n^2 is the *refractive index structure constant* (RISC).

The unit of C_n^2 is $m^{-2/3}$. In the regime of weak turbulence, $C_n^2 \leq 10^{-17}$, while in the regime of strong turbulence, $C_n^2 \geq 10^{-13}$ [10, p. 65]. Accordingly, a larger value of C_n^2 is interpreted being unfavorable. Therefore, from (3), one of the key observations is that appropriately increasing λ would compensate the effects caused by the unfavorable C_n^2 to keep σ_R under an acceptable level. In practice, two wavelengths $\lambda = 0.785$ and $1.55 \mu\text{m}$ are commonly used. Other wavelength could also be used [11].

In the studies of atmospheric turbulence, the effects of σ_R^2 are usually expressed with a pair of induced parameters a and b , to characterize the large-scale and small-scale irradiance fluctuations, respectively. For the spherical wave [10, p. 342],

$$\frac{1}{a} = \exp \left[\frac{0.2\sigma_R^2}{\left(1 + 0.19\sigma_R^{12/5}\right)^{7/6}} \right] - 1, \quad (4)$$

$$\frac{1}{b} = \exp \left[\frac{0.2\sigma_R^2}{\left(1 + 0.23\sigma_R^{12/5}\right)^{5/6}} \right] - 1. \quad (5)$$

V. STATISTICS OF OPTICAL INTENSITY IN STRONG TURBULENCE

Let Z represent the *normalized* irradiance impacted by the composite atmospheric effects. Here “normalized” means $E(Z)=1$, while “composite” covers both large-scale and small-scale effects. According to the *strong fluctuation theory* (SFT) [10, Ch. 9], Z is a random variable following the *gamma-gamma* (GG) distribution with the *probability density function* (PDF) expressed as follows:

$$\begin{aligned} f_Z(z) &= \frac{2(ab)^{(a+b)/2}}{\Gamma(a)\Gamma(b)} z^{(a+b)/2-1} K_{a-b}(2\sqrt{abz}) \\ &= \frac{ab}{\Gamma(a)\Gamma(b)} G_{02}^{20} \left(abz \left| \begin{matrix} - \\ a-1, b-1 \end{matrix} \right. \right), \end{aligned} \quad (6)$$

where $K_\nu(\bullet)$ is the *modified Bessel function of the second kind of order ν* , and $G_{pq}^{mn}(\bullet)$ is *Meijer's G-function* [12, Sec. 9.3]. The conversion is based on [12, eq. (9.34.3)]. The elaboration of Z is given in the following section. Based on (6), we can derive the *cumulative distribution function* (CDF) of Z :

$$\begin{aligned} F_Z(z) &= \frac{(abz)^b \Gamma(a-b)}{b\Gamma(a)\Gamma(b)} {}_1F_2(b; 1-a+b, b+1; abz) \\ &\quad + \frac{(abz)^a \Gamma(b-a)}{a\Gamma(a)\Gamma(b)} {}_1F_2(a; 1+a-b, a+1; abz), \end{aligned} \quad (7)$$

where $a \neq \text{integer}$, $b \neq \text{integer}$, and ${}_1F_2(\cdot)$ is the *generalized hypergeometric function* (GHF).

VI. RELAY SYSTEM MODEL

In the receiver of OWC the *signal-to-noise ratio* (SNR) is a fundamental metric. With the notion of Z defined in the preceding section, the actual received *optical* power in the concerned OWC system can be expressed as:

$$Z_R = P_R Z. \quad (8)$$

where P_R was given in (1). For each symbol, the *converted electrical current* at the detector can be expressed as

$$\mu = RZ_R = RP_R Z. \quad (9)$$

It is worth noting that the electrical current corresponds to the optical power. For the OWC system equipped with the OOK intensity modulator in the transmitter part, the power per symbol (i.e., bit in OOK) of received electrical signal, averaged over the OFF and the transmitted ON signals, is

$$P_s = \frac{\mu^2}{2} = \frac{1}{2} (RP_R Z)^2. \quad (10)$$

According to (10), the instantaneous electrical SNR is:

$$U = \frac{P_s}{2\sigma_N^2} = \frac{R^2 P_R^2 Z^2}{4\sigma_N^2} = U_0 Z^2, \quad (11)$$

where $U_0 = R^2 P_R^2 / (4\sigma_N^2)$. Note that U_0 can be interpreted as the electrical SNR without turbulence. Therefore, Z^2 corresponds to the channel gain in the RF fading channels. From (7) and (11), we can derive the CDF of U as follows:

$$\begin{aligned} F_U(u) &= F_Z \left(\sqrt{\frac{u}{U_0}} \right) \\ &= \frac{(ab)^b \Gamma(a-b)}{b\Gamma(a)\Gamma(b)} \left(\frac{u}{U_0} \right)^{b/2} {}_1F_2 \left(b; 1-a+b, b+1; ab \sqrt{\frac{u}{U_0}} \right) \\ &\quad + \frac{(ab)^a \Gamma(b-a)}{a\Gamma(a)\Gamma(b)} \left(\frac{u}{U_0} \right)^{a/2} {}_1F_2 \left(a; 1+a-b, a+1; ab \sqrt{\frac{u}{U_0}} \right). \end{aligned} \quad (12)$$

The corresponding PDF is:

$$\begin{aligned} f_U(u) &= \frac{1}{2\sqrt{uU_0}} f_Z \left(\sqrt{\frac{u}{U_0}} \right) \\ &= \frac{(ab)^{(a+b)/2}}{\Gamma(a)\Gamma(b)U_0^{(a+b)/4}} u^{[(a+b)/4]-1} K_{a-b} \left(2\sqrt{ab\sqrt{\frac{u}{U_0}}} \right). \end{aligned} \quad (13)$$

The availability of PDF in (13) paves the way to derive the *ergodic capacity* (EC):

$$C_U = \frac{1}{\ln 2} \int_0^\infty \ln(1+u) f_U(u) du. \quad (14)$$

According to [13, p.637, eq. (8.4.6.5)] or [14]:

$$\ln(1+u) = G_{22}^{12} \left(u \left| \begin{matrix} 1 & 1 \\ 1 & 0 \end{matrix} \right. \right). \quad (15)$$

Furthermore, with the aid of a pivotal formula in [15], we can derive a closed-form expression of EC as follows:

$$\begin{aligned} C_U &= \frac{2^{a+b-2}}{\pi \Gamma(a)\Gamma(b) \ln 2} \\ &\quad \times G_{6,2}^{1,6} \left(\frac{16U_0}{(ab)^2} \left| \begin{matrix} 1-a & 2-a & 1-b & 2-b \\ 2 & 2 & 2 & 2 \end{matrix} \right. \right), \end{aligned} \quad (16)$$

Note that the Meijer's G-function is already supported by most software toolkits, including Matlab.

In the cooperative communication systems, there are two classes of protocols: *decode-and-forward* (DF) and *amplify-and-forward* (AF). In DF, the *relay node* (RN) decodes the received signal, re-encodes it, and forwards it to the destination node. In AF, the RN only amplifies the received signal and forwards it to the destination. Analysis and practice have shown that the DF protocol can work well even in the region of low SNR. Therefore, DF is favored by most paradigms.

As shown in Fig. 1, we conduct the analysis for the DF system with three links: S2R link, R2D link, and S2D link. The electrical SNRs experienced at the corresponding receivers are denoted as (U, V, W) . The CDF of V or W has the same structure as that of U in (12). For example,

$$F_V(v) = \frac{(ab)^b \Gamma(a-b)}{b\Gamma(a)\Gamma(b)} \left(\frac{v}{V_0}\right)^{b/2} {}_1F_2\left(b; 1-a+b, b+1; ab\sqrt{\frac{v}{V_0}}\right) + \frac{(ab)^a \Gamma(b-a)}{a\Gamma(a)\Gamma(b)} \left(\frac{v}{V_0}\right)^{a/2} {}_1F_2\left(a; 1+a-b, a+1; ab\sqrt{\frac{v}{V_0}}\right). \quad (17)$$

The operation of this system is based on the repetition coding ([16, pp. 3067-3068], [17]), due to its low complexity for implementation and ease of exposition.

The communication procedures are carried out in two consecutive time slots. In the first time slot, the source node transmits. Then, in the second time slot, the relay node transmits while the source node is idle. This protocol ensures that, in the second time slot, the destination node does not receive two signals simultaneously. This is a fundamental condition that, in all links, the communication signals have the same frequency. If we use subscripts "1" and "2" to explicitly express the time slots for concerned SNRs, then the above protocol implies: $V_1 \equiv 0$ and $W_2 \equiv 0$. Moreover,

$U_1 \neq 0$ since the relay node must receive a signal in the first time slot, otherwise it cannot play a role to equivalently provide an extra source in the second time slot.

In the following, two standard relaying schemes, denoted as Scheme 1 and Scheme 2, are described first. Then, we propose Scheme 3 as a new scheme.

[Scheme 1] In the first timeslot, when the source transmits, only the relay nodes receives. In the second timeslot, the source is idle and only the relay node transmits the signals to the destination.

Denote X as the end-to-end SNR. In this case, it is easy to obtain:

$$X = \min(U_1, V_2). \quad (18)$$

Consequently, the *complementary cumulative distribution function* (CCDF) of X is:

$$r_1(x) = \Pr(X > x) = \Pr[\min(U_1, V_2) > x] = \Pr(U_1 > x)\Pr(V_2 > x) = [1 - F_{U_1}(x)][1 - F_{V_2}(x)], \quad (19)$$

where $F_{U_1}(x)$ and $F_{V_2}(x)$ were given in (12) and (17), respectively. The subscripts "1" and "2" correspond to the first and second time slots, respectively. Since the CDF corresponds to the *outage probability*, the CCDF $r_1(x)$ is equivalent to the *coverage probability* or *reliability*.

[Scheme 2] In the first timeslot, when the source transmits, both relay and destination nodes receive. In the second timeslot, the source is idle and only the relay node transmits the signals to the destination. Therefore, the destination node receives two versions of signals. If the *maximal-ratio combining* (MRC) is adopted in the receiver, then the end-to-end SNR X can be expressed as:

$$X = \min(U_1, Y), \quad (20)$$

where

$$Y = V_2 + W_1. \quad (21)$$

Accordingly, the reliability of X can be expressed as follows:

$$r_2(x) = \Pr(X > x) = \Pr[\min(U_1, Y) > x] = \Pr(U_1 > x)\Pr(Y > x). \quad (22)$$

It is worth mentioning that there is a subtle issue in (22). A true insight could be gained if eq. (22) is rewritten as follows:

$$F_X(x) = \Pr(X \leq x) = 1 - \Pr(U_1 > x)\Pr(Y > x) = \Pr(U_1 \leq x) + \Pr(U_1 > x)\Pr(V_2 + W_1 \leq x). \quad (23)$$

Note that the CDF $F_X(x)$ is just the outage probability of the concerned system. The first term in eq. (23) implies that, if the source-relay channel is poor, then the destination will concede outage, no matter whether $\Pr(W_1 > x)$ or $\Pr(W_1 \leq x)$.

It is instructive to evaluate the differential reliability of Scheme 2 against Scheme 1:

$$\begin{aligned} \Delta r_{21}(x) &= r_2(x) - r_1(x) \\ &= \Pr(U_1 > x)\Pr(Y > x) - \Pr(U_1 > x)\Pr(V_2 > x) \\ &= \Pr(U_1 > x)[F_{V_2}(x) - F_Y(x)] \\ &= \Pr(U_1 > x)[\Pr(V_2 \leq x) - \Pr(V_2 + W_1 \leq x)]. \end{aligned} \quad (24)$$

In (24), we have

$$\begin{aligned} &\Pr(V_2 \leq x) - \Pr(V_2 + W_1 \leq x) \\ &= \int_0^x f_{V_2}(v)dv - \int_0^x F_{W_1}(x-v)f_{V_2}(v)dv \\ &= \int_0^x [1 - F_{W_1}(x-v)]f_{V_2}(v)dv > 0. \end{aligned} \quad (25)$$

As a result, $\Delta r_{21}(x) > 0$.

As shown in (21), Scheme 2 involves the sum of two random variables. In the problem under investigation, according to (17) and the PDF of W , the CDF of Y can be expressed as follows:

$$\begin{aligned} F_Y(y) &= \frac{(ab)^b \Gamma(a-b)}{b\Gamma(a)\Gamma(b)} \frac{(ab)^{(a+b)/2}}{\Gamma(a)\Gamma(b)V_0^{b/2}W_0^{(a+b)/4}} \\ &\times \int_0^y (y-w)^{b/2} {}_1F_2\left(b; 1-a+b, b+1; ab\sqrt{\frac{y-w}{V_0}}\right) \\ &\times w^{[(a+b)/4]-1} K_{a-b}\left(2\sqrt{ab\sqrt{\frac{w}{W_0}}}\right) dw \\ &+ \frac{(ab)^a \Gamma(b-a)}{a\Gamma(a)\Gamma(b)} \frac{(ab)^{(a+b)/2}}{\Gamma(a)\Gamma(b)V_0^{a/2}W_0^{(a+b)/4}} \\ &\times \int_0^y (y-w)^{a/2} {}_1F_2\left(a; 1+a-b, a+1; ab\sqrt{\frac{y-w}{V_0}}\right) \\ &\times w^{[(a+b)/4]-1} K_{a-b}\left(2\sqrt{ab\sqrt{\frac{w}{W_0}}}\right) dw. \end{aligned} \quad (26)$$

It is possible to evaluate (26) by the *moment generating function* (MGF) (i.e., the Laplace transform). According to (6), the MGF of $f_V(v)$ is:

$$M_V(s) = \frac{2^{a+b-2}}{\pi\Gamma(a)\Gamma(b)} G_{1,4}^{4,1} \left(\frac{a^2 b^2}{16sV_0} \left| \begin{matrix} 0 \\ a-2, a-1, b-2, b-1 \end{matrix} \right. \right). \quad (27)$$

The derivation of (27) is based on [18, eq. (16)]. The details are omitted here due to the space limit. The MGF of $f_W(w)$ has a similar expression. Consequently, the CDF of $Y = V_2 + W_1$ (21) can be evaluated through the product $M_V(s)M_W(s)/s$.

Scheme 2 is a standard approach adopted in the RF communications [17]. However, we argue that the reliability of Scheme 2 can be improved by a new scheme, as described below.

[Scheme 3] The transmission sequence is still the same as Scheme 2. Namely, in the first timeslot, the source transmits, while both relay and destination nodes receive. In the second timeslot, the source is idle and only the relay node transmits the signals to the destination. However, here we introduce a new protocol: the destination will concede outage when both $\Pr(U_1 \leq x)$ and $\Pr(W_1 \leq x)$. In other words, if $\Pr(U_1 \leq x)$ while $\Pr(W_1 > x)$, then the destination will still recognize a success. The rationale is that the SNR of the signal directly coming from the source node is strong enough. In this case, we have:

$$F_X(x) = \Pr(U_1 \leq x) \Pr(W_1 \leq x) + \Pr(U_1 > x) \Pr(V_2 + W_1 \leq x). \quad (28)$$

The corresponding differential reliability is:

$$r_3(x) = 1 - F_X(x) = 1 - \Pr(U_1 \leq x) \Pr(W_1 \leq x) - \Pr(U_1 > x) \Pr(V_2 + W_1 \leq x). \quad (29)$$

The reliability gain of Scheme 3 against Scheme 2 is:

$$\Delta r_{32}(x) = r_3(x) - r_2(x) = F_{U_1}(x)[1 - F_{W_1}(x)] > 0. \quad (30)$$

Note that, due to (12) and the same CDF for W , here the differential reliability given in (30) has a closed-form expression, which brings a significant convenience to performance evaluation.

It should be mentioned that Scheme 3 is one of the main contributions of this paper. The following remarks would help gain more insights:

Remark 1: In the theoretical aspect, Scheme 3 stems from the analysis for a two-dimensional marginal distribution function in the three-dimensional space of random variables. Moreover, the correlation feature can be easily introduced. However, the omission of these advanced discussions does

not affect the intuitive descriptions such as eqs. (28) through (30).

Remark 2: In the application aspect, Scheme 3 is not restricted to OWC.

VII. NUMERICAL RESULTS

The numerical experiments are conducted to show the effect of strong turbulence. The main parameter values are: $C_n^2 = 10^{-13}$, $d_p = 700$ or 1000 (m), $\lambda = 0.785$ or 1.55 (μm). Based on these values, the parameter a and b are calculated from (4) and (5). For simplicity, we use the normalized value $U_0 = V_0 = W_0 = 1$. The reliability profiles for Scheme 2 are illustrated in Figs. 2 and 3, where the abscissa is the reliability threshold. The performance can be compared from different aspects. First, the longer wavelength yields the higher reliability. This is particularly obvious in the low SNR threshold regime. Secondly, increasing the link distance from 700 m to 1000 m does not cause much impact. On the other hand, the benefits of the new scheme (Scheme 3) over the conventional scheme (Scheme 2) are illustrated in Figs. 4 and 5. First, it is observed that the improvement is more significant for the shorter wavelength. Secondly, the maximum improvements occur in the similar regime of SNR thresholds.

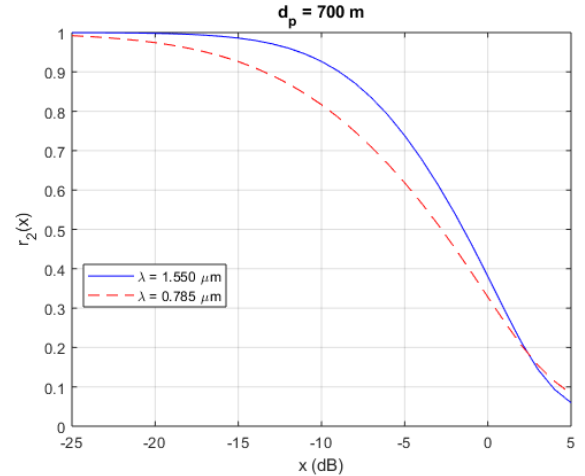


Figure 2. Profile 1 of reliability of Scheme 2.

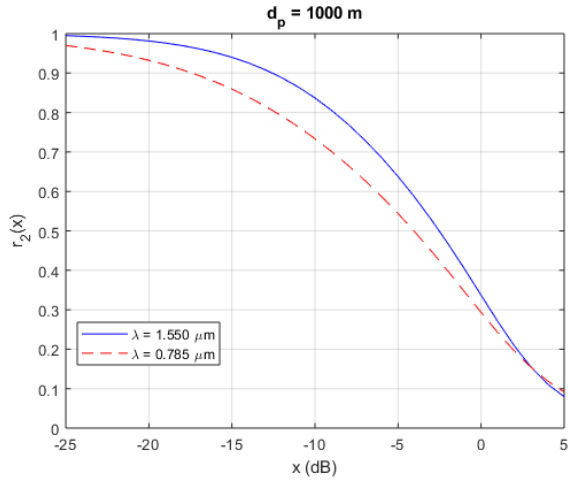


Figure 3. Profile 2 of reliability of Scheme 2.

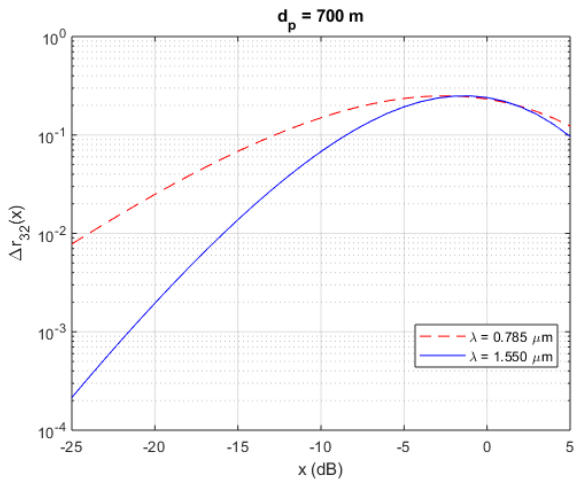


Figure 4. Profile 1 of differential reliability.

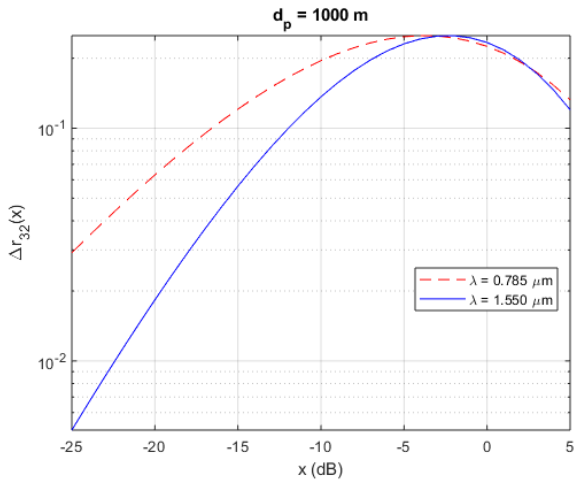


Figure 5. Profile 2 of differential reliability.

VIII. CONCLUSION

In this study, we investigate an OWC segment aided with UAVs. This segment consists of three links, S2R, R2D, and S2D. The channels are subject to the strong turbulence that follows the gamma-gamma distribution. In the discussion of relay protocols, we intentionally elaborated several subtle issues, which were not usually clearly explained in the literature of cooperative communications. Particularly, we introduced Scheme 3. It is one of the main contributions of this paper. Scheme 3 has some rich analytical features and, obviously, its application is not restricted to OWC.

REFERENCES

- [1] M. Z. Chowdhury, Md. T. Hossan, A. Islam, and Y. M. Jang, "A comparative survey of optical wireless technologies: architectures and applications," *IEEE Access*, vol. 6, pp. 9819-9840, January 2018.
- [2] M. Mozaffari, W. Saad, M. Bennis, Y.-H. Nam, and M. Debbah, "A tutorial on UAVs for wireless networks: applications, challenges, and open problems," *IEEE Communications Surveys & Tutorials*, vol. 21, no. 3, pp. 2334-2360, 2019.
- [3] A. Fotouhi, H. Qiang, M. Ding, M. Hassan, L. G. Giordano, A. Garcia-Rodriguez, and J. Yuan, "Survey on UAV cellular communications: practical aspects, standardization advancements, regulation, and security challenges," *IEEE Communications Surveys & Tutorials*, vol. 21, no. 4, pp. 3417-3442, 2019.
- [4] J. M. Kahn and J. R. Barry, "Wireless infrared communications," *Proc. of the IEEE*, vol. 85, pp. 265-298, 1997.
- [5] R. Otte, L. de Jong, and A. van Roermund, *Low-Power Wireless Infrared Communications*, Kluwer Academic Publishers, Boston, 1999.
- [6] C. C. Chen and C. S. Gardner, "Impact of random pointing and tracking errors on the design of coherent and incoherent optical intersatellite communication links," *IEEE Transactions on Communications*, vol. 37, no. 3, pp. 252-260, 1989.
- [7] J. J. Degnan and B. J. Klein, "Optical antenna gain. 2: receiving antennas," *Applied Optics*, vol. 13, no. 10, pp. 2397-2401, 1974.
- [8] J. C. Palais, *Fiber Optic Communications* (5th ed.), Prentice Hall, 2005.
- [9] K. A. Winick, "Atmospheric turbulence-induced fades on optical heterodyne communications links," *Applied Optics*, vol. 25, no. 11, pp. 1817-1825, 1986.
- [10] L. C. Andrews and R. L. Phillips, *Laser Beam Propagation through Random Media*, SPIE Press, 2005.
- [11] X. Liu, "Free-space optics optimization models for building sway and atmospheric interference using variable wavelength," *IEEE Transactions on Communications*, vol. 57, no. 2, pp. 492-498, 2009.
- [12] I. S. Gradshteyn and I. M. Ryzhik, *Table of Integrals, Series, and Products* (7th ed.), Academic Press, 2007.
- [13] A. P. Prudnikov, Y. A. Brychkov, and O. I. Marichev, *Integrals and Series, Volume 3: More Special Functions*. New York, NY, USA: Gordon and Breach Science Publishers, 1990.
- [14] <http://functions.wolfram.com/HypergeometricFunctions/MeijerG/03/01/03/23/>
- [15] <http://functions.wolfram.com/HypergeometricFunctions/MeijerG/21/02/07/>
- [16] J. N. Laneman, D. N. C. Tse, and G. W. Wornell, "Cooperative diversity in wireless networks: efficient protocols and outage behavior," *IEEE Transactions on Information Theory*, vol. 50, no. 12, pp. 3062-3080, 2004.
- [17] A. F. Molisch, *Wireless Communications* (2nd Ed.), Hoboken, NJ: Wiley, 2010.
- [18] X. Liu, "Closed-form expressions of ergodic capacity in cloud radio access networks with Nakagami-m fading," *IEEE Transactions on Vehicular Technology*, vol. 66, no. 12, pp. 11430-11434, December 2017.